Studies of the Phase Structure of Poly(tetramethylene oxide) by VT/MAS ^{13}C NMR

Asako Hirai,* Fumitaka Horii, and Ryozo Kitamaru

Institute for Chemical Research, Kyoto University, Uji 611, Japan

José Gómez Fatou and Antonio Bello

Instituto de Plasticos y Caucho, Juan de la Cierva 3, E-28006 Madrid, Spain

Received October 4, 1989; Revised Manuscript Received December 12, 1989

ABSTRACT: The phase structure of poly(tetramethylene oxide) (PTMO) crystallized from the melt was investigated at −100 to 0 °C using high-resolution solid-state ^{13}C NMR with a variable-temperature/magic-angle spinning system. By using the differences in the longitudinal and transverse magnetic relaxation times, we found that solid PTMO consists of a crystalline phase, a crystalline–amorphous interphase, and an amorphous phase. For the crystalline component the α-methylene resonance, appearing at 72.9 ppm, exhibits two different T_{1C}'s, 209 and 9.3 s, at 0 °C. In contrast, the resonances related to the amorphous and interfacial components, which are at 70.9 and 72.0 ppm, respectively, display the same T_{1C} of 0.15 s but different T_{2C} values of 7.8 and 0.099 ms, respectively. Similar results are obtained for the β-methylene carbon. The line-shape analysis of the total spectrum containing all the components shows that the mass fractions of the crystalline component, the crystalline–amorphous interphase, and the amorphous phase are 0.60, 0.22, and 0.18, respectively. The lamellar thickness is determined as 145 Å from SAXS. From these values, thicknesses of the crystalline, interfacial, and amorphous components are estimated to be 87, 16, and 26 Å, respectively.

Introduction

Solid-state high-resolution ^{13}C NMR spectroscopy is a powerful technique for characterizing the structures of crystalline and noncrystalline regions in semicrystalline polymers. In a previous paper[1] the phase structure of lamellar crystalline polyethylene was investigated by high-resolution solid-state ^{13}C NMR. It was revealed that the polyethylene samples isothermally crystallized at 129 or 130 °C from the melt consist of not only the crystalline and amorphous phases but also a crystalline–amorphous interphase which differ distinctly in ^{13}C chemical shift as well as spin–spin relaxation time T_{2C}.

In this paper the phase structure of linear poly(tetramethylene oxide) (PTMO) crystallized from the melt is studied by using almost the same high-resolution solid-state ^{13}C NMR technique as exploited for polyethylene[1-3] and polypropylene.[4]

Experimental Section

Sample. PTMO was prepared by ring-opening polymerization of tetrahydrofuran by using triethyloxonium hexafluoroantimonate in methylene chloride at 0 °C. The number-average molecular weight, which was determined with a Hewlett-Packard 502 high-speed membrane osmometer at 28 °C in toluene, is 67 000.

The sample was melted at 65 °C and then crystallized at 20 °C for 1 month. After the sample was kept at 23 °C for 3 months, the NMR spectra were measured.

DSC Measurements. The fusion curves for the sample were obtained on a Mettler TA-3000 with a DSC-30 head at a heating rate of 5 °C min^{-1}.

Carbon-13 NMR Measurements. CP/MAS ^{13}C NMR measurements were performed at −100 to 0 °C on a JEOL JNM-FX200 spectrometer operating at 4.7 T equipped with a variable-temperature/magic-angle spinning (VT/MAS) system. Magic-angle spinning at 3.0 kHz was used throughout this work. Hartmann–Hahn matched fields with strengths $\gamma B_1/2\pi$ of 62.5 kHz were applied to ^{13}C and ^{1}H nuclei, and the ^{1}H radiofrequency strength was reduced to 54.3 kHz during ^{1}H dipolar decoupling (DD). The recycle time after collection of the FID was 10 s. ^{13}C chemical shifts relative to tetramethylsilane were determined by using the CH_2 line at 32.89 ppm of the crystalline component of polyethylene as an external reference.

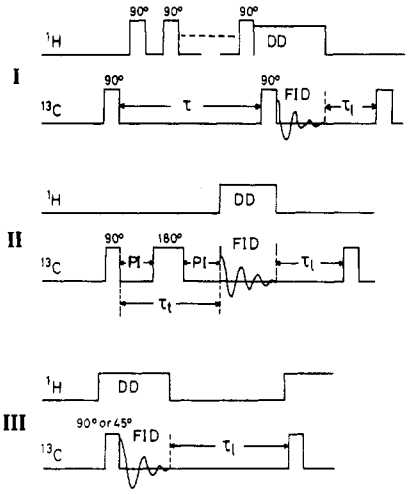

Figure 1. Pulse sequences used in this work: (I) saturation–recovery method modified for measurements in a solid; (II) pulse sequence for ^{13}C T_2 measurements; (III) single-pulse sequence.

T_{1C} values longer than a few seconds were measured by using the CPT1 pulse sequence developed by Torchia,[5] while T_{1C}'s shorter than a few seconds were measured by the saturation–recovery pulse sequence modified for solid samples without CP. The pulse sequences used for the measurements of shorter T_{1C}'s and T_{2C}'s are shown in diagrams I and II of Figure 1, respectively. Figure 1(III) shows a 90° or 45° single-pulse sequence to obtain ^{13}C NMR spectra without CP. If the waiting time τ_1 after the acquisition of an FID is appropriately set, one can obtain partially or fully relaxed spectra that reflect part or all of the components included in the sample.

The temperature shown in this report is the apparent temperature indicated by the JEOL temperature control unit. Our preliminary calibration suggests an underestimation of ca. 10 °C.

Since the melting point of PTMO is 42 °C and partial melting occurs at 30 °C, all NMR measurements in the solid state were made at or below 0 °C in this work.

0024-9297/90/2223-2913$02.50/0

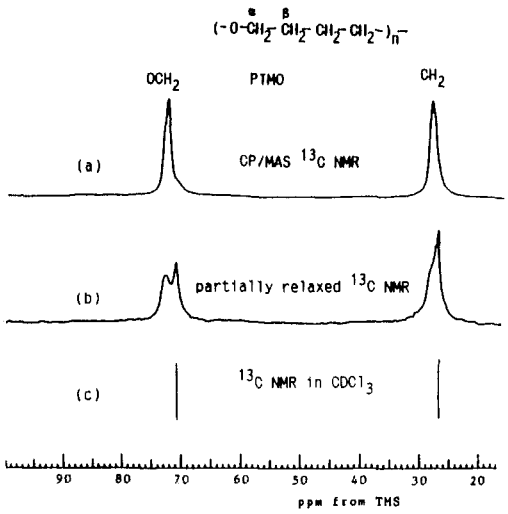

Figure 2. (a) CP/MAS ^{13}C NMR spectrum of PTMO at 0 °C. (b) Partially relaxed ^{13}C NMR spectrum of PTMO at 0 °C. (c) ^{13}C NMR spectrum of PTMO in $CDCl_3$ at room temperature.

X-ray Scattering Measurements. The long period of the PTMO sample was determined by small-angle X-ray scattering measurement, using 6-m SAXS (Franks-type point-focusing camera)[6] at the High Intensity X-ray Laboratory of Kyoto University.

Results and Discussion

Figure 2a shows the 50-MHz CP/MAS ^{13}C NMR spectrum of PTMO at 0 °C. PTMO possesses two different kinds of carbon atom within the monomeric unit, α-methylene (OCH_2) and β-methylene (CH_2), as shown in this figure. The downfield and upfield resonances are assigned to α-methylene and β-methylene carbons, respectively. The α-methylene resonance line seems to be composed of a large peak at 72.9 ppm and an upfield broader shoulder. These contributions must be the crystalline and noncrystalline components, respectively, but the intensity of the noncrystalline component may be significantly reduced because of the lower CP efficiency of the noncrystalline component. In order to locate the resonances belonging to the noncrystalline component, a 50-MHz ^{13}C NMR spectrum of PTMO at 0 °C was measured by a 90° single-pulse sequence (pulse sequence III) as shown in Figure 2b. τ_1 was set to 5 s in order to emphasize the noncrystalline component by reducing the contribution from the crystalline component with longer T_{1C}'s compared to those of the noncrystalline component. Another sharp line is clearly seen somewhat upfield for each resonance. The chemical shifts of these upfield lines correspond well to those of PTMO obtained in deuterated chloroform solution which are shown as the stick-type scalar-decoupled ^{13}C NMR spectrum in Figure 2c. Therefore we simply assign here the upfield and downfield lines to the noncrystalline and crystalline components, respectively. The detailed assignment will be given later. The chemical shifts of the α- and β-methylene carbons are listed in Table I together with the chemical shifts measured for PTMO in solution.

In order to know the molecular mobility of the crystalline and noncrystalline components, we have measured the ^{13}C spin–lattice relaxation time T_{1C} using either the CPT1 pulse sequence or the saturation–recovery method (pulse sequence I) and the ^{13}C spin–spin relaxation time T_{2C} using pulse sequence II. Figure 3 shows the semilogarithmic decay curve of the peak intensity for the crystalline resonance line at 72.9 ppm in the ^{13}C spin–lattice relaxation measured by the CPT1 pulse sequence. If the sample contains several components with different T_{1C}'s, the total ^{13}C magnetization $M_C(t)$ measured at time t is given by

$$M_C(t) = 2\sum M_{CP,i} \exp(-t/T_{1C,i})$$

Here, $M_{CP,i}$ is ^{13}C magnetization of component i generated by the CP procedure. As clearly seen in Figure 3, two-component analysis by a computer has confirmed the existence of two components with different T_{1C}'s (209 and 9.3 s). Here, the data for the short-T_{1C} component, which are shown as squares in Figure 3, were obtained by subtracting the extrapolated values of the long-T_{1C} component (the upper straight line) from the observed values shown by open circles. Since the partially relaxed spectra measured by the CPT1 pulse sequence contain no upfield noncrystalline component, both T_{1C} components should be assigned to the crystalline components. In contrast, the noncrystalline line at 70.9 ppm has a single T_{1C} of 0.15 s as shown in Figure 4. Here, the recovery process of the magnetization of the noncrystalline line, which was obtained by pulse sequence I, was analyzed by a computer using a least-square method.

Figure 5 shows a semilogarithmic plot of the peak height of the line at 70.9 ppm as a function of τ_t during the ^{13}C transverse relaxation, which was measured by pulse sequence II with τ_1 = 3.5 s. Here, the contribution from the crystalline components to the noncrystalline component was estimated to be negligibly small, because only 9% of the total crystalline component appears at τ_1 = 3.5 s and, furthermore, the noncrystalline line is separated by 2 ppm from the crystalline line. The overall decay curve (the upper line in Figure 5) can be clearly resolved into two parts, a rapid decay within 0.1 ms and a subsequent slow decay. The slope of the slower decay yields T_{2C} = 7.95 ms, and the T_{2C} of the rapid decay is estimated to be 0.099 ms by the usual two-component decay analysis.

Table I
^{13}C Chemical Shifts, T_1's, and T_2's of PTMO at 0 °C

	chem shift/ppm	T_1/s	T_2/ms
OCH_2	72.9	209,[a] 9.3[a]	
	70.9	0.15[b]	7.95, 0.099
	(70.64)[c]		
CH_2	28.3	209,[a] 10.4[a]	
	27.0	0.14[b]	8.22, 0.099
	(26.56)[c]		

[a] Obtained by Torchia's pulse sequence. [b] Obtained by saturation–recovery method. [c] In $CDCl_3$.

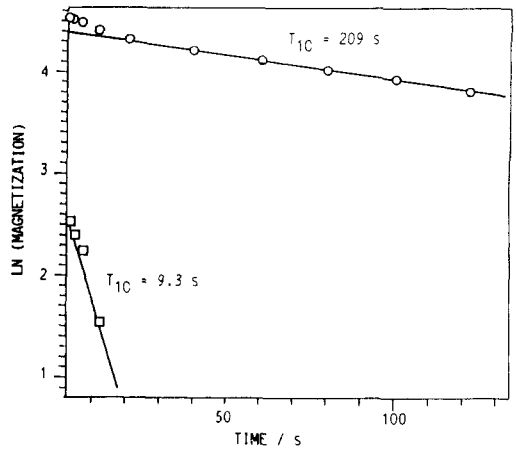

Figure 3. Semilogarithmic plots of ^{13}C spin–lattice relaxation time T_{1C} measured by Torchia's pulse sequence as a function of t for the crystalline α-methylene carbon.

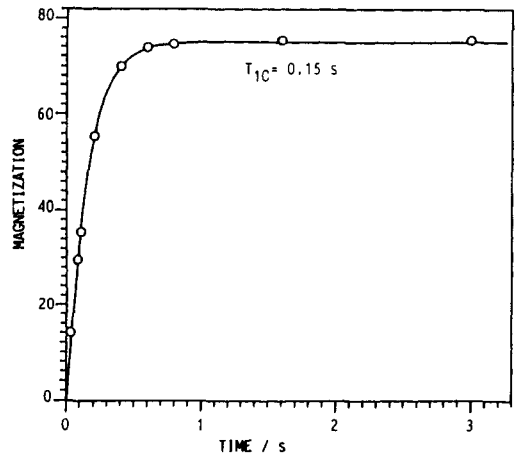

Figure 4. Semilogarithmic plot of T_{1C} measured by saturation–recovery as a function of τ for the noncrystalline α-methylene carbon.

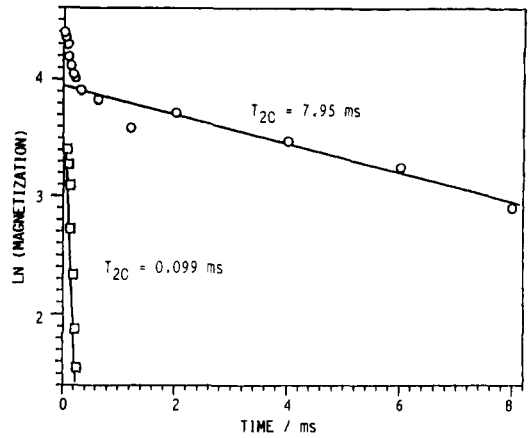

Figure 5. Semilogarithmic plots of spin–spin lattice relaxation time T_{2C} as a function of τ_t.

T_{1C}'s and T_{2C}'s at 0 °C thus estimated for both the α- and β-methylene carbons are also summarized in Table I. These results show that within the crystalline regions, both methylene carbons possess two components with different T_{1C}'s. On the other hand, the noncrystalline regions consist of two phases with different T_{2C} values but have the same T_{1C} value. This behavior is similar to that displayed by the polyethylene samples.[1-3] In order to investigate further the noncrystalline regions with two different T_{2C}'s, we have applied the same technique as in the case of polyethylene samples.[1]

Figure 6a shows the spectrum obtained for the α-methylene carbons using pulse sequence I with τ = 0.8 s. This spectrum arises from the whole noncrystalline region because the τ value is set to be longer than $5T_{1C}$ for this component. Although 1.7% of the crystalline component with T_{1C} = 209 and 9 s is also contained in this line, such a small contribution may be negligible.

Figure 6b shows the spectrum obtained for the α-methylene carbon utilizing pulse sequence II with τ_t = 600 μs and τ_1 = 3.5 s. This spectrum shows only the contribution from the noncrystalline component with a longer T_{2C}, since the noncrystalline component with the shorter T_{2C} (99 μs) disappears under this condition. Moreover, as described above, the chemical shift (70.9 ppm) of this component is close to that observed for this polymer in solution. Consequently, this line can be assigned to the noncrystalline component with a rubber-like mobility as in the case of polyethylene.[1]

Spectrum c in Figure 6, which is obtained by subtracting the rubbery component (Figure 6b) from the whole

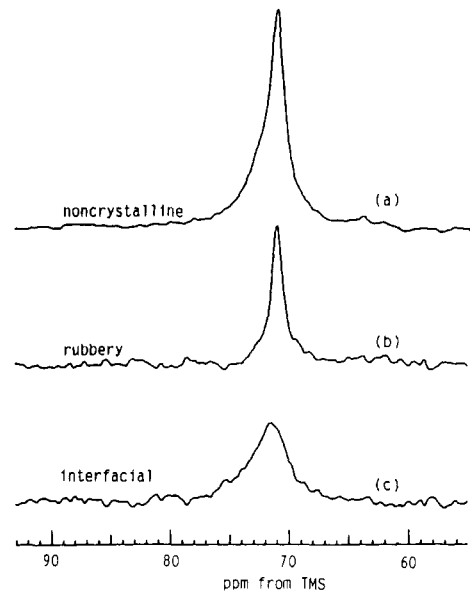

Figure 6. (a) Partially relaxed spectrum of α-methylene carbon at 0 °C measured by pulse sequence I with τ_1 = 0.8 s. (b) Partially relaxed spectrum of α-methylene carbon measured by pulse sequence II with τ = 600 μs and τ_1 = 3.5 s. (c) The (a)–(b) difference spectrum.

noncrystalline component (Figure 6a), is assigned to the interfacial component, although 7% of the crystalline component may appear as downfield tailing. This assignment is based on the value of the somewhat larger chemical shift and the short T_{2C} of 99 μs in analogy with the case of polyethylene. The interfacial component has the same T_{1C} as for the rubbery component but a shorter T_{2C} compared to that of the rubbery component. T_{1C} is associated with chain motion on the order of 10^8 Hz, while T_{2C} may be determined by a slower molecular motion with 10^4–10^5 Hz if such motion exists. Accordingly, the interfacial component should be discriminated from the rubbery component by the difference in somewhat long range motion with a lower frequency, whereas these two components would not be distinguished from each other in shorter range motion with a higher frequency possibly associating with several backbone atoms. As in the case of polyethylene samples crystallized from the melt,[1] the PTMO sample is therefore concluded to consist of three regions: the crystalline region, the noncrystalline interfacial region with limited molecular mobility, and the noncrystalline interzonal region with a rubber-like pronounced molecular mobility.

In order to determine the mass fractions of the crystalline, the interfacial, and the rubbery components, we have measured the fully relaxed ^{13}C NMR spectrum of the PTMO sample at 0 °C by a 45° single-pulse sequence (pulse sequence III), as shown in Figure 7a. Here, the recycle time τ_1 was chosen to be 600 s in order to obtain the contributions from all structural components. Figure 7b shows the spectrum of the crystalline component recorded with the CPT1 pulse sequence by setting the delay time t = 2.56 s for the longitudinal relaxation. Although this spectrum comprises two crystalline components with T_{1C}'s of 9.3 and 209 s, the resonance line can be well assumed to be a single Lorentzian. The total spectrum in Figure 7a has been analyzed in terms of three Lorentzians that well describe the spectra of the respective components shown in Figures 6b, 6c, and 7b using a least-squares method: the line width and the peak height of each component have been varied while keeping the peak position of 72.9, 72.0, and 70.9 ppm constant. The

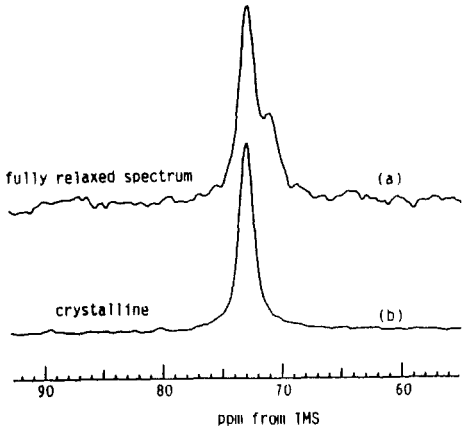

Figure 7. (a) Fully relaxed ^{13}C NMR spectrum of PTMO (τ_1 = 600 s). (b) Spectrum of the crystalline component.

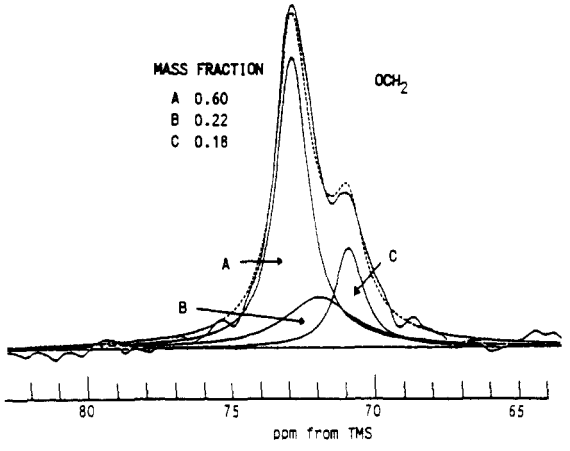

Figure 8. Component analysis of the total spectrum of α-methylene carbon shown in Figure 7a: (A) crystalline component; (B) interfacial component; (C) rubbery component.

result is shown in Figure 8, where the integrated intensity fractions of the respective components are also shown. It is seen that the composite curve indicated by the dotted line reproduces well the observed spectrum. The integrated intensity fraction of the crystalline line is 0.60. The degree of crystallinity can also be obtained from separate calorimetric measurements if the heat of fusion ΔH_u for the 100% crystalline sample is known. The heat of fusion of this PTMO sample was estimated to be 8.13 kJ/mol by DSC together with the melting temperature of 42 °C as a peak temperature. Since ΔH_u is 14.2 kJ/mol for PTMO,[7] the degree of crystallinity is estimated to be 0.57. This value is in excellent accord with the integrated intensity fraction of the crystalline line shown in Figure 8. This fact therefore reconfirms the assignments of the 72.9 ppm line to the crystalline components and then the other lines at 72.0 and 70.9 ppm to the noncrystalline components. According to the X-ray analysis, PTMO crystallizes in a planar zigzag conformation.[8,9] The chemical shift of the interfacial component (72.0 ppm) is significantly close to that of the crystalline component (72.9 ppm), suggesting that the interfacial component has a trans-rich conformation compared to the amorphous component, although this conformation must be motionally averaged by the rapid gauche–trans transition. The shorter T_{2C} of the interfacial component compared to that of the rubbery component may also support the trans-rich conformation for the former component.

To estimate the thickness of each phase, we measured the long period of PTMO by SAXS. When the lamella

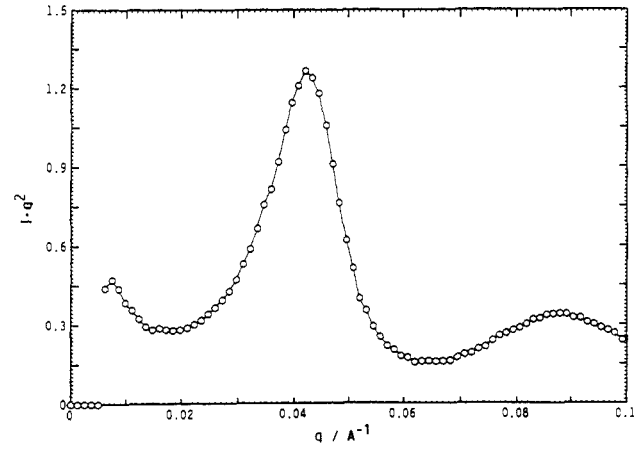

Figure 9. SAXS curve for PTMO. I = scattering intensity, q = scattering vector, $q = (4\pi/\lambda) \sin\theta$, λ = wavelength, and 2θ = scattering angle.

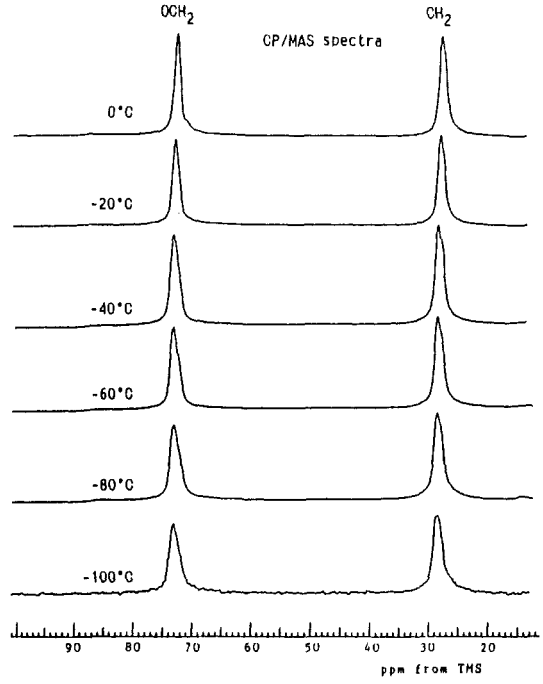

Figure 10. CP/MAS ^{13}C NMR spectra of PTMO at different temperatures.

is assumed to be a flat disk,[10] it may be convenient to plot Iq^2 against q as shown in Figure 9. Here, I and q are scattering intensity and scattering vector, respectively. The first- and second-order peaks are clearly seen, indicating a regular stacking of lamellae. The long period is estimated as 145 Å. The thickness of the crystalline, interfacial, and noncrystalline components are estimated to be 87, 16, and 26 Å, respectively, using the degree of crystallinity and the long period. The thickness of the interfacial component thus obtained is in good accord with the theoretical value deduced by Flory et al.[11] and the experimental result obtained by small-angle neutron scattering analysis.[12,13] Nevertheless, the interfacial region of PTMO is significantly thinner than that of bulk-crystallized polyethylenes with M_v = 20 000–110 000 whose thicknesses are 34 Å.[1] This means that the molecular chains of PTMO with C–O–C bonds may be more flexible compared to the molecular chains of polyethylene with C–C bonds.

Figure 10 shows CP/MAS ^{13}C NMR spectra for PTMO obtained at −100 to 0 °C. With decreasing temperature, each resonance line shifts downfield accompanying the increase in line width. The results are summarized in

Table II
Chemical Shifts and Line Widths of α- and β-Methylene Carbons of PTMO at Various Temperatures by CP/MAS ^{13}C NMR

temp,[a] °C	α-methylene chem shift/ppm	α-methylene Δν/Hz	β-methylene chem shift/ppm	β-methylene Δν/Hz
0	72.9	71.4	28.3	78.6
-20	72.9	78.6	28.3	78.6
-40	73.1	72.9	28.5	85.7
-60	73.1	100.0	28.6	92.9
-80	73.2	107.1	28.6	100.0
-100	73.3	114.3	28.7	100.0

[a] Temperature is the instrumental temperature.

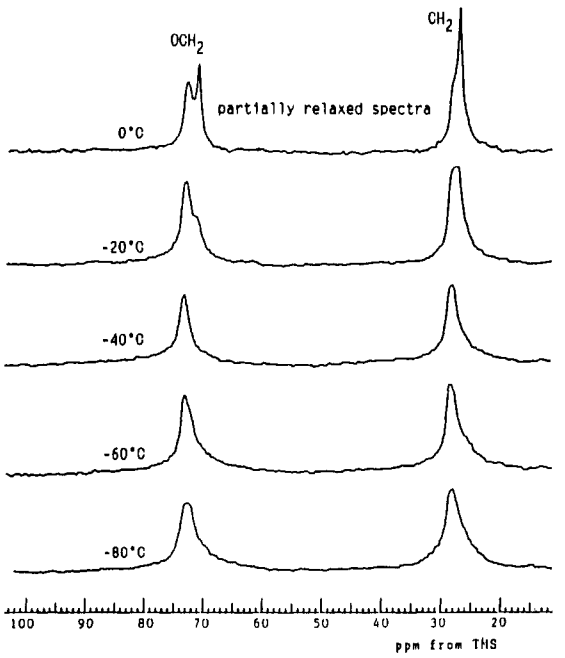

Figure 11. Partially relaxed ^{13}C NMR spectra of PTMO at different temperatures (τ_1 = 5 s).

Table II. In these spectra the upfield shoulder of α-methylene carbon tends to disappear below -20 °C. To obtain the signal of the noncrystalline component, we have measured ^{13}C NMR spectra by a 90° single pulse (pulse sequence III) with τ_1 = 5 s as shown in Figure 11. The noncrystalline component that is clearly observed at 70.9 ppm at 0 °C disappears below -40 °C, possibly because of the line broadening. Such a line-broadening process may correspond to the glass transition process of PTMO that is observed by ^{13}C NMR spectroscopy.

One of the causes of the disappearance of the upfield noncrystalline component in the CP/MAS spectra shown in Figure 10 is found to be line broadening of this component, possibly due to the limitation of the enchanced liquid-like motion or the reduction in the efficiency of the dipolar decoupling by the onset of the motion with the same order of frequency as the decoupling field. A similar disappearance of the noncrystalline line was observed in CP/DD ^{13}C NMR spectra at -13 to -90 °C of solid polyethylene.[14] In that case the proton spin-lattice relaxation time $T_{1\rho H}$ in the rotating frame was reduced to 2-3 ms at -75 and -95 °C from 38 ms at 30 °C. Such reduction in $T_{1\rho H}$ should result in the decrease of the CP efficiency and then a decrease in ^{13}C signal intensity. Probably the $T_{1\rho H}$ is also decreased for the noncrystalline component of PTMO at these lower temperatures, suggesting that such a decrease should be another cause of the disappearance of the noncrystalline line at lower temperatures. This will be examined in future separate experiments.

Conclusions

1. The phase structure of poly(tetramethylene oxide) (PTMO) crystallized from the melt has been elucidated by high-resolution solid-state ^{13}C NMR with a variable-temperature/magic-angle spinning system as being composed of the crystalline, interfacial, and rubbery components.

2. Examination of the partially relaxed ^{13}C NMR spectra in the longitudinal and transverse directions reveals that the α-methylene resonance line consists of a crystalline component at 72.9 ppm, an interfacial component at 72.0 ppm, and an amorphous component at 70.9 ppm. These two noncrystalline components can also be discriminated by the significant difference in T_{2C}, indicating much different local molecular mobility between them.

3. The mass fractions of the crystalline, the interfacial, and the amorphous components are determined to be 0.60, 0.22, and 0.18, respectively, by the line-shape analysis of the total spectrum. Thicknesses of the crystalline, interfacial, and amorphous components are estimated to be 87, 16, and 26 Å, respectively, from the mass fractions and the long period.

Acknowledgment. We thank Dr. Hisao Hayashi of the Department of Polymer Chemistry, Faculty of Engineering, Kyoto University, for obtaining the long period of the PTMO sample by SAXS.

References and Notes

(1) Kitamaru, R.; Horii, F.; Murayama, K. *Macromolecules* **1986**, *19*, 636.
(2) Zhu, Q.; Horii, F.; Tsuji, M.; Kitamaru, R. *J. Soc. Rheol. Jpn.* **1989**, *17*, 35.
(3) Nakagawa, M.; Horii, F.; Kitamaru, R. *Polymer*, **1990**, *31*, 323.
(4) Saito, S.; Moteki, Y.; Nakagawa, M.; Horii, F.; Kitamaru, R. *Polym. Prepr. (Am. Chem. Soc., Div. Polym. Chem.)* **1988**, *29* (1), 6; *Macromolecules*, in press.
(5) Torchia, D. A. *J. Magn. Reson.* **1978**, *30*, 613.
(6) Hayashi, H.; Hamada, F.; Suehiro, S.; Ogawa, T.; Miyaji, H. *J. Appl. Crystallogr.* **1988**, *21*, 330.
(7) Flory, P. J. *Principles of Polymer Chemistry*; Cornell University Press: Ithaca, NY, 1953.
(8) Imada, K.; Miyakawa, T.; Chatani, Y.; Tadokoro, H.; Murahashi, S. *Makromol. Chem.* **1965**, *83*, 113.
(9) Cesari, M.; Perego, C.; Mazzei, A. *Makromol. Chem.* **1965**, *83*, 196.
(10) Guinier, A.; Fournet, G. *Small-Angle Scattering of X-rays*; Wiley: New York, 1955; p 21.
(11) Flory, P. J.; Yoon, D. Y.; Dill, K. A. *Macromolecules* **1984**, *17*, 862.
(12) Flory, P. J.; Yoon, D. Y. *Nature (London)* **1978**, *272*, 226.
(13) Yoon, D. Y. *J. Appl. Crystallogr.* **1978**, *11*, 531.
(14) Nakagawa, M.; Saito, S.; Horii, F.; Kitamaru, R. *Polym. Prepr., Jpn* **1987**, *36*, 987.